Journal of Thermal Analysis and Calorimetry, Vol. 56 (1999) 1461-1473

PRE-EUTECTIC DENSIFICATION OF CALCIUM CARBONATE DOPED WITH LITHIUM CARBONATE

F. Tétard, D. Bernache-Assollant and E. Champion

Laboratoire de Matériaux Céramiques et Traitements de Surface, UPRESA CNRS 6015
123, Avenue Albert Thomas, 87060 Limoges Cedex, France

Abstract

Pressureless sintering of $CaCO_3$ was carried out, with Li_2CO_3 (from 0.5 to 8 wt%) as an additive, under different pressures of CO_2. Densification occurs between 600 and 700°C. Sintering above the eutectic temperature (T>662°C) leads to the decomposition of calcium carbonate and the materials become expanded. At 620° under 1 kPa of CO_2, a relative density of 96% is reached. Li_2CO_3 enhances the densification process and grain growth of calcium carbonate. CO_2 pressure slows down densification and grain growth kinetics. These results are explained by the influence of carbonate and calcium ion vacancies on the sintering mechanisms.

Keywords: $CaCO_3$, densification, kinetics, Li_2CO_3

Introduction

Natural calcium carbonate (i.e. coral, aragonite structure) is currently used as a bone substitute in orthopaedic surgery [1–3]. The sintering of synthetic calcite could be an attractive way to extend the potential applications because a controlled and adapted microstructural design of the implant material could be performed. Thus, it appears interesting to investigate the sintering mechanisms of calcite. In this field, few studies have been devoted to the sintering of $CaCO_3$, may be because its thermal instability is a difficulty to overcome in the elaboration of dense synthetic calcium carbonate. For instance, $CaCO_3$ decomposes into CaO from 550°C in air and from 890°C under a pressure of 100 kPa of CO_2 gas. Therefore, the elaboration of dense $CaCO_3$ materials requires thermal treatments at low temperature under controlled atmosphere of CO_2 to prevent decomposition. To this end, hot pressing techniques and/or the addition of sintering aids may appear useful to enhance densification process of $CaCO_3$. Tullis [4] and Olgaard [5–7] used hot isostatic pressing under 500 MPa of argon at a temperature comprised between 650 and 900°C to densify natural (Solnhofen) or pure $CaCO_3$ up to a relative density of 96% of the theoretical value. Yamasaki [8–11] used hydrothermal hot pressing in order to lower the temperature required to densify $CaCO_3$ below 350°C. But, because with this elaboration technique pores are filled with water which cannot be totally removed, the relative density of materials did not exceeded 90%. The addition of sintering aids to promote liquid phase sintering appeared as an alternative processing route. Urabe [12] showed that the

1418–2874/99/ $ 5.00

Akadémiai Kiadó, Budapest
Kluwer Academic Publishers, Dordrecht

addition of some lithium based compounds (LiF, Li_3PO_4), which are able to form a liquid phase with $CaCO_3$, allowed an effective densification (up to $d \approx 83\%$ d_{th}).

We have demonstrated in a previous paper that, in the presence of lithium phosphate as sintering aid, $CaCO_3$ could be nearly fully densified by solid phase sintering at a temperature below the eutectic temperature between $CaCO_3$ and Li_3PO_4 [13].

From these bases, the present work is concerned with pressureless sintering of calcium carbonate with lithium carbonate as sintering aid. Lithium carbonate being known to form a liquid phase with $CaCO_3$ at the eutectic temperature of 662°C [14], the study will show that similarly to Li_3PO_4, the addition of Li_2CO_3 allows to densify $CaCO_3$ providing the sintering temperature remains below the eutectic point. The influence of CO_2 pressure during sintering and of the amount of added Li_2CO_3 on the relative density and grain size of $CaCO_3$ are also investigated.

Materials and methods

Materials

Calcium carbonate powder (Aldrich Company) contained 40.04 wt% of calcium, corresponding to 99.995% pure calcite (supplier data). Specific surface area, measured by the BET method was 1.00 $m^2\ g^{-1}$ (Surface analyser Micromeritics ASAP-2010, 8 points). The agglomerate size distribution (Micromeritics particle sizer) was comprised between 0.6 and 30 μm and average size was 2 μm. Lithium carbonate was supplied by Merck. It was 99.99% pure (supplier data). This powder had a specific surface area of 0.81 $m^2\ g^{-1}$ and an average grain size of 1.25 μm.

The amount of Li_2CO_3 added to $CaCO_3$ varied from 0 to 8 wt%. The two powders ($CaCO_3$, Li_2CO_3) were mixed in pure ethanol during 15 min. The mixing was performed in an alumina container. The blended powders were dried at 100°C during 24 h. Then, disks of 10 mm diameter and 2.5 mm thick were uniaxially pressed under a stress of 125 MPa and compacts were pressureless sintered in a CO_2 atmosphere.

Characterisation techniques

Thermogravimetric analysis was performed on pure and mixed powders using a Setaram B85 thermobalance (precision 10 μg). The heating rate was 10°C min^{-1} and the CO_2 atmosphere was kept at the constant pressure of 100 kPa.

Dilatometric measurements were registered on pressed disks using a Setaram TMA92 dilatometer. CO_2 gas pressure varied between 0.5 and 100 kPa. The heating rate was 10°C min^{-1} to determine sample shrinkage *vs.* temperature. Isothermal measurements of shrinkage were also performed. In this case, samples were heated at 40°C min^{-1} up to the dwelling temperature.

Relative density of sintered materials was determined by the Archimedes method in water. Theoretical density of samples was calculated using a single mixture rule of the starting powder data, theoretical density of $CaCO_3$ and Li_2CO_3 being 2.71 and 2.90 g cm^{-3} respectively.

Microstructural observations were performed by scanning electron microscopy (SEM) on a Philips XL 30 apparatus. Before observation, samples were polished with a 1 μm diamond paste to obtain a mirror like surface. To reveal the microstructure, these surfaces were thermally etched by heating during 2 min at 570°C under 100 kPa CO_2. Grain size analysis was performed using a commercial software (Grafek, Optilab 2.6). Grain size distribution of each sample was determined from the analysis of at least 600 grains issued from 3 different images. The grain size or equivalent disk diameter (G) was calculated from the measurement of grain surface (A), on the hypothesis of spherical grains, using the following equation :

$$G = 2\sqrt{\frac{A}{\pi}}$$

X-ray diffraction patterns (XRD) were registered using a Siemens D5000 diffractometer (CuK_α radiation, 2θ range 22°–85° step scan 0.01, step time 10 s). Crystalline phases were determined from comparison with the JCPDS reference data file. Lattice parameters were calculated using 19 diffraction peaks by the least-squares method (Diffract AT software, Pseudo-Voigt function).

Results

Thermal stability

Thermogravimetric analysis was performed under a 100 kPa CO_2 pressure, which corresponds to a theoretical temperature of 890°C for $CaCO_3$ decomposition. Figure 1 shows that the decomposition of pure $CaCO_3$ starts from the same temperature of 890 and is completed at 975°C. The maximum mass loss is 44.0% and corresponds to the theoretical value for total decomposition.

With 8 wt% of added Li_2CO_3, the mass loss begins at about 600 and becomes significant from 890°C. The decomposition is completed at 925°C. A small mass loss of

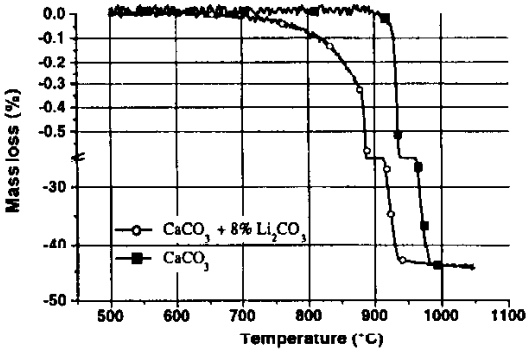

Fig. 1 TG analysis of pure and 8 wt% Li_2CO_3-doped $CaCO_3$ powders (100 kPa CO_2)

about 0.35% is registered below 890°C which cannot be attributed to the decomposition of pure powders. Calcium carbonate remains stable up to that temperature and fusion without any decomposition up to 1000°C was registered for pure lithium carbonate. This means that this mass loss should be linked to the incorporation of Li_2CO_3 in $CaCO_3$ whose mechanism will be discussed hereafter.

Dilatometric analysis

Figure 2 gives linear shrinkage *vs.* temperature increase (P_{CO_2}=100 kPa) for pure and 8 wt% Li_2CO_3-doped $CaCO_3$. For pure calcite, the sintering begins at 600°C. Nevertheless, shrinkage remains low up to 890°C and the final relative density only reaches 66% of the theoretical value.

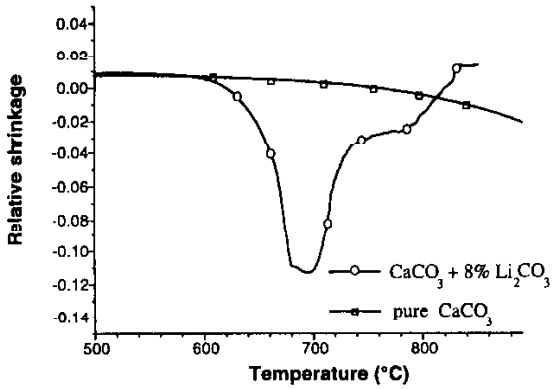

Fig. 2 Shrinkage of pure and 8 wt% Li_2CO_3-doped $CaCO_3$ samples *vs.* temperature under 100 kPa CO_2

A very different behaviour is obtained in the presence of Li_2CO_3. In this case, two distinct domains can be observed:

(i) between 600 and 700°C, the shrinkage registered on the samples corresponds to an important densification. This densification occurs by solid phase sintering below 660° and liquid phase sintering above that temperature which corresponds to the eutectic point between $CaCO_3$ and Li_2CO_3 (T_e=662°C). From 660°C, the liquid phase appears and is accompanied with an increase of densification rate. This higher sintering rate results from an easier rearrangement of grains in the presence of liquid and from an activation of densification by dissolution mechanism at grain boundaries. Nevertheless, isothermal experiments performed in this temperature range (660–700°C) pointed out an expansion of samples indicating a beginning of calcite decomposition.

(ii) above 700°C, a linear expansion is registered. This expansion is accompanied with a dedensification process. $CaCO_3$ starts to decompose (a mass loss of about 0.02% being registered at 700°C, Fig. 1) and the liquid phase induces the formation

pores. These pores, which size can be larger than 100 μm, and the associated expansion, can be attributed to decomposition gas which remains imprisoned inside the samples.

From these results, it appears that the elaboration of dense calcite by pressureless sintering should be conducted in a temperature range below the eutectic point to prevent any expansion by gas imprisonment induced by the simultaneous presence of a liquid phase and a beginning of calcite decomposition. Consequently, a temperature of 620° has been chosen for sintering experiments.

Sintering

Influence of Li_2CO_3 addition

$CaCO_3$ containing 0, 0.5, 2 and 8 wt% Li_2CO_3 were pressureless sintered at 620°C during 9 h under a 1 kPa CO_2 gas pressure (equilibrium pressure of CO_2 at 620°C being 0.4 kPa). Relative density and average grain size of these materials are given in Table 1.

Table 1 Characteristics of sintered materials (620°C. 9 h. P_{CO_2}=1 kPa)

Li_2O_3/wt%	0	0.5	2	8
Density/g cm^{-3}	1.626	2.507	2.605	2.613
Relative density/% d_{th}	60.0	92.5	96.0	95.9
Average grain size/μm	1.76±0.03	70±1.6	17.0±0.5	9.0±0.3

Without Li_2CO_3 addition, neither density nor grain size of calcium carbonate are modified after thermal treatment. These results agree with those found by Olgaard [7] indicating that for pure calcite no microstructural changes occurred below 700°C. On the contrary, the addition of Li_2CO_3 greatly influences the final density and microstructure.

With 0.5 wt% Li_2CO_3, a high relative density is obtained and an important grain growth is observed with an average grain size of about 40 times that measured in pure calcite. Moreover, as shown in Fig. 3, this exaggerated growth induces the formation of needle-like grains, whereas spherical-like grains remain in pure calcite. XRD analysis (Fig. 4) shows an increase in the intensity of peaks attributed to (0 0 6) and (0 0 12) reticular planes. This indicates that grains grow preferentially along C-axis. The presence of Li_2CO_3 does not modify the crystal structure of calcite (JCPDS n° 4-486) but induces an increase of lattice parameters (Table 2). This phenomenon has also been observed by Rajam [15] in lithium doped $CaCO_3$ crystals synthesised by precipitation (a=4.997 Å; c=17.097 Å).

A higher Li_2CO_3 loading (≥2 wt%) leads to a smaller average grain size and to a higher relative density of sintered materials (d=96%). The presence of inclusions in calcite being known to restrict grain growth [16–17], the limited grain growth in these materials can be associated to the presence of Li_2CO_3 precipitates at $CaCO_3$ grain boundaries, as shown in Fig. 5. And, as opposed to materials containing

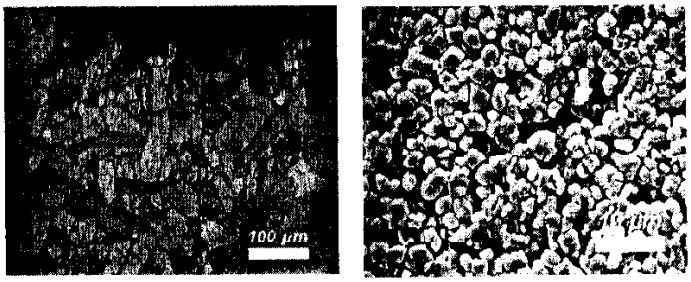

Fig. 3 SEM micrographs of samples sintered at 620°C, 15 h, 1 kPa CO_2; a – 8 wt% Li_2CO_3-doped $CaCO_3$; b – pure $CaCO_3$

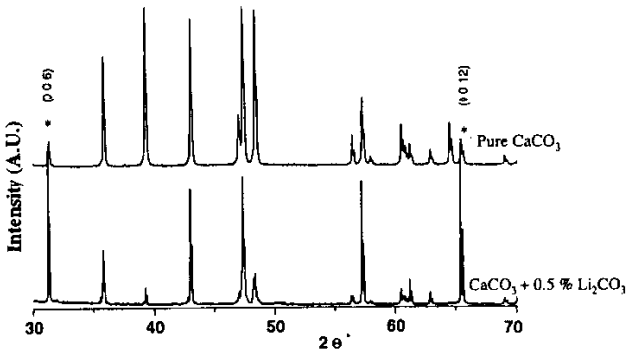

Fig. 4 XRD patterns of pure and 0.5 wt% Li_2CO_3-doped $CaCO_3$ sintered materials

Table 2 Lattice parameters of sintered calcite (620°C, 9 h P_{CO_2}=1 kPa)

$CaCO_3$+0.5 wt% Li_2CO_3	pure $CaCO_3$
a=0.4991±0.001 Å	a=4.989±0.001 Å
c=17.065±0.004 Å	c=17.059±0.004 Å

0.5 wt% Li_2CO_3 in which such precipitates were not observed, grain growth appears normal. Grain size distribution of $CaCO_3$-2 wt% Li_2CO_3 materials sintered at 620°C for different times and of materials with different amounts of Li_2CO_3 sintered at the same temperature during 9 h confirm normal grain growth. Results are plotted in Figs 6 and 7, respectively. In these figures, G_i represents the average size of grains of class i and $\overline{G}$ the average size for the whole population. Figures 6a and 7a show that grain growth remain normal whatever the sintering time or amount of Li_2CO_3 might be. Moreover, grain size distributions are self-similar, i.e. they are totally

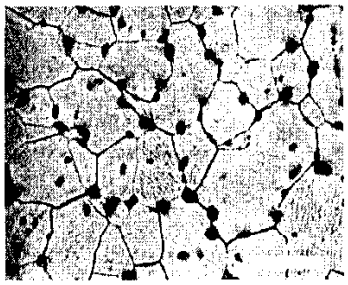

Fig. 5 SEM (Backscattered electron image) of 2 wt% Li_2CO_3-doped $CaCO_3$ material showing Li_2CO_3 precipitates at grain boundaries (in dark)

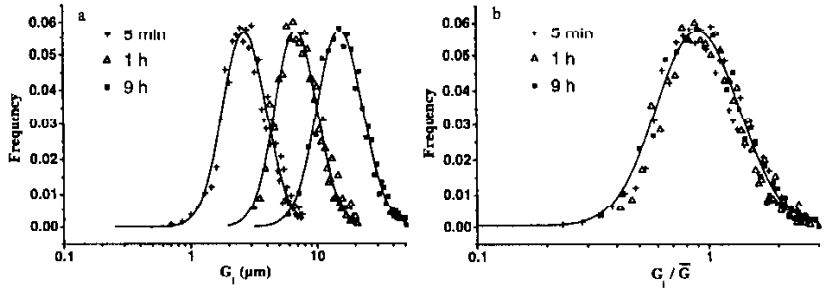

Fig. 6. Grain size distribution of 2 wt% Li_2CO_3-doped $CaCO_3$ *vs.* sintering time (620°C, 1 kPa CO_2)

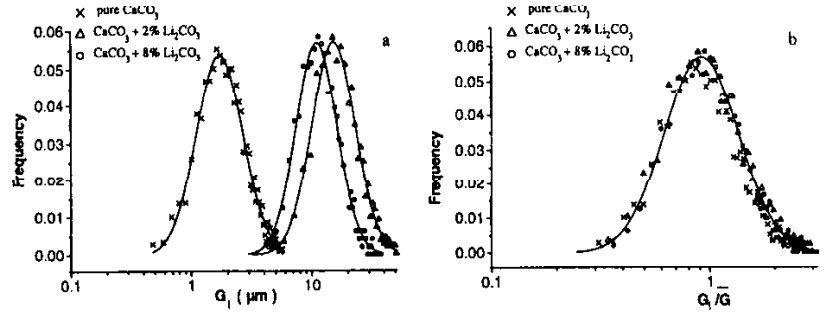

Fig. 7 Grain size distribution pure and doped $CaCO_3$ (sintering: 620°C, 9 h, 1 kPa CO_2)

identical when expressed in the reduced co-ordinate system $G_i/\overline{G}$ (Figs 6b and 7b). Such a behaviour has already been described by several authors [18–20]. Therefore, a stationary phenomenon is reached from 2 wt% Li_2CO_3. This means that the function which describe grain size distribution $G=f(G_i, t)$ can be transformed in a law in

which G_i and t are separate variables: $G=f(G_i, t)=g(G_i/\overline{G}(t))$. This also allows to justify the use of average grain size ($\overline{G}$) as unique variable to characterise grain growth kinetics.

Average grain size *vs.* sintering time (under 1 kPa CO_2) for materials containing 2 and 8 wt% Li_2CO_3 are given in Fig. 8. The plot shows an asymptotic behaviour and a grain growth decrease for increasing amount of Li_2CO_3. The growth is inhibited from a limiting grain size G_l of $12^{\pm 2}$ and $25^{\pm 5}$ μm for 8 and 2 wt% of Li_2CO_3, respectively.

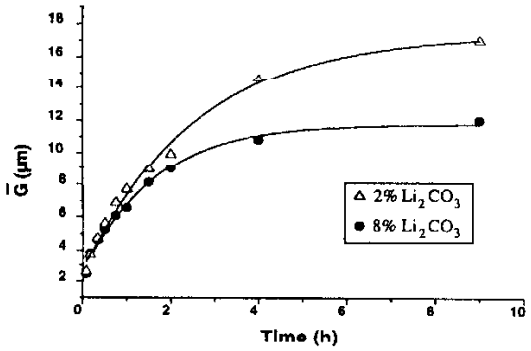

Fig. 8 Average grain size of doped $CaCO_3$ *vs.* sintering time (620°C, 1 kPa CO_2)

Influence of CO_2 gas pressure

This part of the study has been performed using 2 wt% Li_2CO_3-doped $CaCO_3$ sintered at 620°C under a CO_2 gas pressure varying from 1 to 100 kPa. The relative density of sintered materials is given in Fig. 9. Under high CO_2 pressure, the final relative density does not exceed 90% of the theoretical value whereas it is always higher for pressures closer to the equilibrium value ($P_{CO_{2eq}}$=0.4 kPa at 620°C). In the same time, the average grain size of calcite decreases with the increase of CO_2 pressure (Fig. 10).

Discussion

The effect of Li_2CO_3 addition on the pre-eutectic sintering of $CaCO_3$ (i.e. solid phase sintering at $T<T_e$) can be explained by the formation of a solid solution between Li_2CO_3 and $CaCO_3$. Youdri [21] has already pointed out the presence of lithium (0.05 wt%) in interstitial site inside the calcite lattice in single crystals of an eutectic composition of Li_2CO_3–$CaCO_3$. The following reaction can be proposed to describe the incorporation of lithium in calcite:

$$Li_2CO_3 \xrightarrow{CaCO_3} 2Li_i^{\circ} + V''_{Ca} + CO^{x}_{3_{CO_3}} \qquad \text{(R 1)}$$

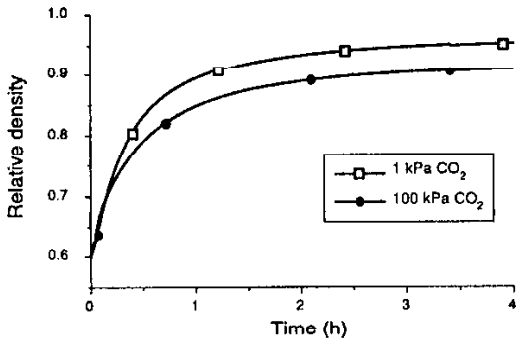

Fig. 9 Influence of CO_2 gas pressure on relative density of 2 wt% Li_2CO_3-doped $CaCO_3$ sintered at 620°C, 9 h

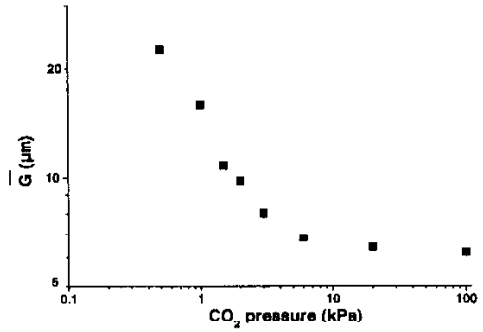

Fig. 10 Influence of CO_2 gas pressure on calcite grain size of 2 wt% Li_2CO_3-doped $CaCO_3$ sintered at 620°C, 9 h

According to (R1), below the solubility threshold, the concentration of calcium ion vacancies increases whereas that of carbonate ion vacancies decreases with lithium carbonate incorporation. Above the solubility threshold, defects concentrations should remain constant. Figures 11a and 11b give qualitative plots of these concentrations in the case of a high and low lithium ion solubility, respectively.

On this basis, two cases must be distinguished depending on whether the amount of added lithium carbonate exceeds the solubility threshold of lithium ion or not.

(i) At low Li_2CO_3 content a total solubility of added Li_2CO_3 in $CaCO_3$ can be hypothesised.

Our results obtained on 0.5 wt% Li_2CO_3-doped $CaCO_3$ agree with this hypothesis. The formation of the solid solution is accompanied by an increase of the concentration of calcium ion vacancies. As experimentally, both densification and grain growth of calcium carbonate were enhanced by the addition of Li_2CO_3, calcium ion vacancies are the rate controlling species in the sintering mechanisms of calcium

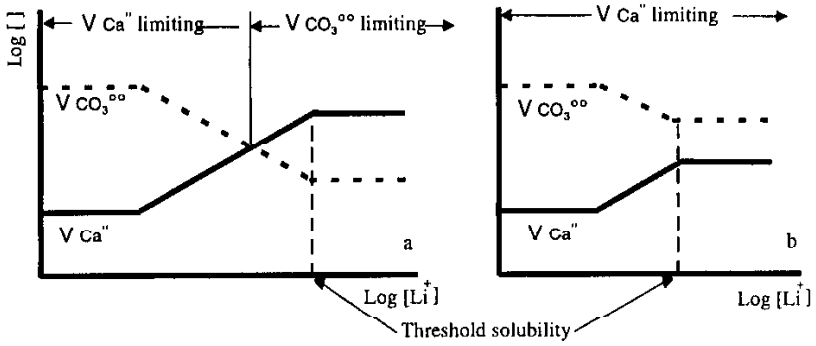

Fig. 11 Schematic plot of Ca^{2+} and CO_3^{2-} vacancies *vs.* Li^+ concentration; a. High solubility of lithium carbonate, b. Low solubility of lithium carbonate

carbonate. Similar results were found by Farver [22] who demonstrated through diffusion experiments that calcium ion is the specie which diffuses at the lowest rate in pure calcite. Moreover, the selective stabilisation of (0 0 1) reticular plane by lithium ion has been verified by Parker [23] through a modelling of calcite grain morphology in the presence of Li^+ and by Titiloye [24] on synthetic crystals. Therefore, an abnormal grain growth must be obtained, which is in accordance with our microstructural observations.

When the amount of incorporated lithium ions increases, the concentration of calcium ion vacancies can increase up to a maximum value, corresponding to the solubility threshold of Li^+, and then remains constant.

(ii) At high content, the solubility threshold is reached and part of the added Li_2CO_3 should remain in excess.

This agrees with the presence of Li_2CO_3 precipitates inducing a limited grain growth, as observed in $CaCO_3$ containing 2 and 8 wt% Li_2CO_3.

A modification of the Zener's law [25] allows to take on account the inhibition of grain growth induced by particles in the case of a preferred distribution of these particles along grain boundaries (i.e. mobile particles) [26]. The limiting size G_l depends on the volume fraction of particles (f) according to the following relationship:

$$G_l = \frac{Kr}{f^{1/2}}$$

where K is a constant ($K=2.8^{\pm 0.1}$) and r the radius of Li_2CO_3 particles (1.25 μm).

As schematised in Fig. 11, two hypotheses can be made to explain the sintering behaviour above the solubility threshold. The rate controlling species may be either carbonate ion vacancies (Fig. 11a) or calcium ion vacancies (Fig. 11b).

Theoretical analysis of densification kinetic indicates that the densification rate can be described by the following relationship [27, 28]:

$$\delta\rho/\delta\tau = CD/G^n \quad (1)$$

where C and n are constants. D is the diffusion coefficient of the rate controlling species and G is the grain size.

According to Eq. (1), a decrease of densification rate may result from two phenomena: an increase of grain size or a decrease of diffusion process. Experimental results obtained on 2 wt% Li_2CO_3-doped $CaCO_3$ *vs.* CO_2 gas pressure for a same thermal cycle must support the right hypothesis, i.e. a decrease of both densification (Fig. 9) and grain size (Fig. 10) with the increase of CO_2 pressure. As grain size decreases with the increase of CO_2 pressure, according to Eq. (1), the simultaneous decrease of densification rate should necessary result from a decrease of diffusion coefficient of the rate controlling species. Consequently, the concentration of these rate controlling species must decrease with the pressure increase.

The beginning of calcite decomposition in the presence of Li_2CO_3 from 600°C also imposes to take the presence of oxygen ions, associated with CO_2 gas release, into account. Nevertheless, if oxygen ions are located in carbonate sites, the concentrations of calcium and carbonate ion vacancies are independent from CO_2 gas pressure. The hypothesis of oxygen ions located in interstitial sites may also be considered. The formation of these defects can be written as follows:

$$CO^x_{3_{CO_3}} + V_i^x \longleftrightarrow O_i'' + V^{oo}_{CO_3} + CO_2 \quad (R\ 2)$$

Due to the very low amount of decomposed $CaCO_3$ below the eutectic temperature, the activity of carbonate vacancies and interstitial oxygen can be assimilated to their concentration (i.e. dilute defects). In the same time, the activity of carbonate ions can be hypothesised as constant, equal to 1. Then, the equilibrium constant for (R 2) is given by:

$$K = [O_i'][V_{CO_3}^{oo}]P_{CO_2} \quad (2)$$

The presence of lithium carbonate gives the following equation for zero charge balance:

$$[Li_i^o] + 2[V^{oo}_{CO_3}] = 2[V''_{Ca}] + 2[O_i''] \quad (3)$$

Moreover, Schottky's equilibrium leads to:

$$\phi \longleftrightarrow V^{oo}_{CO_3} + V''_{Ca} \quad (R\ 3)$$

with:

$$K_s = [V^{oo}_{CO_3}][V''_{Ca}] \quad (4)$$

Finally, using Eqs (2) and (4), the relation given in Eq. (3) can be written as follows:

$$[Li_i^o] + 2[V^{oo}_{CO_3}] = \frac{2K_s}{[V^{oo}_{CO_3}]} + \frac{2K}{[V''_{CO_3}]P_{CO_2}} \quad (5)$$

Solving this second degree equation gives the concentration of carbonate ion vacancies:

$$[V_{CO_3}^{oo}] = \frac{-[Li_i^o] + \sqrt{[Li_i^o]^2 + 16(K_s + (K/P_{CO_2}))}}{4} \quad (6)$$

Figure 12 gives punctual defect concentrations (calcium and carbonate ion vacancies, interstitial oxygen ions) *vs.* CO_2 gas pressure simulated from these equations. Increasing CO_2 gas pressure leads to a decrease of carbonate ion vacancies and to a concomitant increase of calcium ion vacancies. Therefore, in accordance with results above mentioned indicating that the concentration of the rate controlling species must decrease when CO_2 pressure is increased, carbonate ion vacancies constitute the controlling species in the densification and grain growth of Li_2CO_3-doped $CaCO_3$ above the solubility threshold.

Finally, the addition of Li_2CO_3 as sintering aid of $CaCO_3$ leads to a progressive change of kinetic regime: the rate controlling species is calcium ion vacancy at low Li_2CO_3 concentration and becomes carbonate ion vacancy at high Li_2CO_3 concentration. This behaviour corresponds to the case illustrated in Fig. 11a.

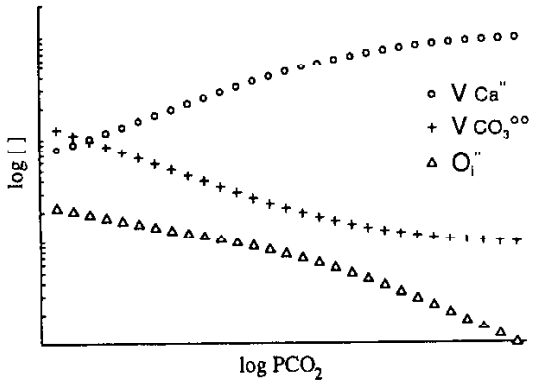

Fig. 12 Simulated plot of vacancies concentrations *vs.* CO_2 gas pressure

Conclusions

This study demonstrates that pressureless sintering of calcium carbonate under CO_2 atmosphere can be performed with Li_2CO_3 as an additive. The use of Li_2CO_3 which forms a liquid phase with $CaCO_3$ at 662°C could have appeared useful to activate densification processes by liquid phase sintering (i.e. sintering at T>662°C). But in this case, though lithium carbonate enhances densification processes, in the same time it facilitates calcite decomposition which starts at lower temperature. Therefore, the elaboration of materials having a high relative density requires a sintering temperature below the eutectic point between Li_2CO_3 and $CaCO_3$ to prevent calcite

decomposition (i.e. solid phase sintering at $T<662°C$). CO_2 gas pressure also influences densification and grain growth kinetics.

Densification mechanisms and grain growth agree with the hypothesis of a partial solubility of lithium carbonate in calcium carbonate. Below solubility threshold, calcium ion vacancy controls densification kinetic. Lithium ions incorporated in calcite lattice stabilise (0 0 1) reticular plane inducing an abnormal grain growth. Above solubility threshold, carbonate ion vacancy controls densification kinetic and grain growth is limited by Li_2CO_3 precipitates which segregate at gain boundaries.

References

1 G. Guillemin, A. Meunier, P. Dallant and P. Christel, J. Bio. Mater. Res., 23 (1989) 765.
2 Y. Fujita, T. Yamamuro, T. Nakamura and S. Kotani, J. Bio. Mater. Res., 25 (1991) 991.
3 H. Ohgushi, M. Okumura, T. Yoshikawa and K. Inoue, J. Bio. Mater. Res., 26 (1992) 885.
4 J. Tullis and R. A. Yund, J. Geology, 90 (1982) 301.
5 D. L. Olgaard and B. Evans, J. Am. Ceram. Soc., 69, 11 (1986) C-272.
6 D. L. Olgaard and B. Evans, Contr. Mineral. Petrol., 100 (1988) 246.
7 D. L. Olgaard and J. D. Fitz Gerald, Contrib. Mineral. Petrol., 115 (1993) 138.
8 N. Yamasaki and T. Weiping, J. Mat. Sci. Let., 12 (1993) 516.
9 N. Yamasaki, T. Weiping, H. Lei and K. Hosoi, J. Mat. Sci. Let., 14 (1995) 1751.
10 N. Yamasaki, T. Weiping and K. Yanagisawa, J. Mat. Res., 8 (1993) 1972.
11 N. Yamasaki, T. Weiping, K. Jiajun and K. Hosoi, J. Mat. Sci. Let., 14 (1995) 1268.
12 K. Urabe, T. Kojima and Y. Goto, J. Ceram. Soc. Jpn., 103 (1995) 1097.
13 F. Tétard, D. Bernache-Assollant, E. Champion and P. Lortholary, Solid State Ionics, 101–103 (1997) 517.
14 W. Eitel and W. Skaliks, Z. Anorg. U. Allgem. Chem., 183 (1929) 268.
15 S. Rajam and S. Mann, J. Chem. Soc., Chem. Commun., (1990) 1789.
16 D. Robinson, Contr. Mineral. Petrol., 32 (1971) 245.
17 D. L. Mas and P. D. Crowley, J. Metamorphic Geol., 14 (1996) 155.
18 W. W. Mullins and J. Vinals, Acta Metal., 37 (1989) 991.
19 P. L. Chen and I. W. Chen, J. Am. Ceram. Soc., 77 (1994) 2289.
20 J. Ricote and L. Pardo, Acta Met., 44 (1996) 1155.
21 L. Youdri, Thesis n°1000, Toulouse, France, June 1981.
22 J. R. Farver and R. A. Yund, Contrib. Mineral. Petrol., 123 (1996) 77.
23 S. C. Parker, E. T. Kelsey, P. M. Oliver and J. O. Titiloye, Faraday Discus., 95 (1993) 75.
24 J. O. Titiloye, S. C. Parker, D. J. Osguthorpe and S. Mann, J. Chem. Soc., Chem. Commun., (1991) 1494.
25 C. Zener, Private communication, Trans. Amer. Inst. Min. (Metal.) Eng., 175 (1949) 15.
26 F. Tétard, Thesis n°16–1997, Limoges, France, June 1997.
27 C. Herring, J. Appl. Phys., 21 (1950) 301.
28 R. L. Coble, J. Appl. Phys., 32 (1961) 787.